Transport in a Lévy ratchet: Group velocity and distribution spread

B. Dybiec* and E. Gudowska-Nowak†
M. Smoluchowski Institute of Physics and Mark Kac Center for Complex Systems Research, Jagellonian University, ul. Reymonta 4, 30-059 Kraków, Poland

I. M. Sokolov‡
Institut für Physik, Humboldt-Universität zu Berlin, Newtonstrasse 15, D-12489 Berlin, Germany
(Received 22 April 2008; published 21 July 2008)

We consider the motion of an overdamped particle in a periodic potential lacking spatial symmetry under the influence of symmetric, white, Lévy noise, being a minimal setup for a "Lévy ratchet." Due to the nonthermal character of the Lévy noise, the particle exhibits a motion with a preferred direction even in the absence of whatever additional time-dependent forces. The examination of the Lévy ratchet has to be based on the characteristics of directionality which are different from typically used measures such as mean current and the dispersion of particle positions, since these become inappropriate when the moments of the noise diverge. To overcome this problem, we discuss robust measures of directionality of transport such as the position of the median of the particle displacement distribution characterizing the group velocity and the interquantile distance giving the measure of the distribution width. Moreover, we analyze the behavior of splitting probabilities for leaving an interval of a given length, unveiling qualitative differences between the noises with Lévy indices below and above unity.

DOI: 10.1103/PhysRevE.78.011117 PACS number(s): 05.40.Fb, 05.10.Gg, 02.50.Ey

I. INTRODUCTION

Motion of particles in systems with external periodic potential with broken spatial symmetry (referred to as ratchets) under the influence of additional external forces with zero mean can result in occurrence of the persistent, directed current [1–5]. Typically, one assumes that the overall force acting on the particle is a superposition of the Gaussian thermal noise with another periodic or stochastic force [4]. In these cases all moments of the distribution of the noisy force do exist, and the existence of moments of the distribution of the particle's velocity is guaranteed.

There are at least two reasons to consider the directed motion of a particle in a periodic ratchet potential under the influence of a heavy-tailed noise causing anomalously large particle displacements. One of them is pursuing the line of investigations of rectification of nonthermal noises and generalizing the corresponding considerations to the heavy-tailed cases which were found to be quite abundant under nonequilibrium conditions [6–9]. Another one, connected with the former, is seeking for a way to characterize the ensuing directed motion in the case when the corresponding statistical moments are absent, so that neither the dispersion nor even the mean of the corresponding displacements exists so that standard characteristics of motion such as mean velocity or Péclet number become inapplicable.

The interplay of deterministic dynamics and Lévy-type noises has been addressed in the literature in various setups. The discussion concentrated on such noise-induced effects as resonant activation [10,11], stochastic resonance [12], dynamical hysteresis [12,13], studies of decay and relaxation properties of the probability densities [14,15], escape from bounded intervals [16,17], the classical barrier crossing problem [18–20], or examination of stationary states [15,21–23]. However, very few works [24] tackle the problem of Lévy-noise-driven dynamics in periodic potentials. In the present work we study the behavior of a particle in the periodic potential with a broken spatial symmetry subjected to a symmetric, white, Lévy-stable noise.

The α-stable Lévy noises constitute a fundamental family of stochastic processes with stationary and independent increments. The occurrence of Lévy motions is naturally anticipated in systems far from thermal equilibrium [25], where detailed balance and microscopic reversibility conditions might be explicitly violated [6]. In such situations, the noise is known to play a dominant role and its interaction with nonlinear dynamics may induce a ratchet effect [4]. Consequently, we discuss here a minimal model of such effects which involves ingredients such as spatial periodicity and random (unbiased) forces. The Lévy-ratchet model considered essentially resembles so-called thermal ratchet [4] with time-dependent temperature variations leading to directed particle current. Heavy tails of the distribution of driving stochastic increments lead, however, to considerable peculiarities of such motion, due to the power-law character of the probability density of the particle displacements, which lack the dispersion and may also lack the mean. Therefore, the examination of the current defined as an ensemble average of velocity over realizations of stochastic dynamics may not be adequate for the Lévy ratchet and other quantities which could characterize the motion induced by the interplay of nonequilibrium driving and nonlinearity of the potential have to be introduced. Here, instead of examining the current and the effective diffusion coefficient, we discuss several robust probabilistic measures based on the cumulative distribution of particles' displacement: the behavior of the median,

*bartek@th.if.uj.edu.pl
†gudowska@th.if.uj.edu.pl
‡igor.sokolov@physik.hu-berlin.de

which allows us to introduce the group velocity, the growth of interquantile distances, and the behavior of splitting probabilities.

Our analysis of the model system asserts that symmetric stable (non-Gaussian) noise acting in the presence of a potential with broken spatial symmetry can induce directed transport of test particles. As long as the mean value of the noise exists (this situation is realized for α-stable noises with the stability index $1<\alpha\leqslant 2$), the displacement of the particle also possesses a mean and the overall motion can be characterized by the temporal changes of the mean position and therefore by the velocity. In contrast, if the noise is distributed according to a Lévy-stable law with $0<\alpha<1$, neither the mean of the noise nor the mean of the overall displacement exists, so that one has to look for other quantities characterizing the motion. The discussion of these quantities, in parallel with investigation of the properties of the directed transport, is the main objective of the present paper. The paper is organized as follows: In the next section (Sec. II) the minimal Lévy-ratchet model is introduced. Section III includes numerical results and discusses various characteristics of the considered ratcheting device. The cumulative distribution of the overall displacement probability is examined in Sec. III A, whereas its main features (such as the median) allowing for a definition of a group velocity of the probability packet are studied in Sec. III B. We discuss also the interquantile distance (Sec. III C), as well as the concept of the splitting probability (Sec. III D) that defines the fraction of particles going to the left (to the right) when leaving an interval of a finite length. Finally, in Sec. III E we analyze properties of the escape time distribution from a box of a given width. The paper ends with a summary and concluding remarks (Sec. IV).

II. LÉVY-RATCHET MODEL

Let us consider a generalized, overdamped Brownian particle in an external potential,

$$V(x)=\frac{1}{2\pi}\left[\sin 2\pi x+\frac{1}{4}\sin 4\pi x\right], \tag{1}$$

with a broken spatial symmetry (see Fig. 1). The system is described by the Langevin equation

$$\frac{dx}{dt}=-V'(x)+\zeta(t), \tag{2}$$

where $\zeta(t)$ stands for a driving white, Lévy-stable noise with independent increments distributed according to the stable density with the index α. In other words, $\zeta(t)$ stands for a generalized white noise process being the time derivative of the corresponding Lévy-Brownian Markovian-stable process [7,16,22,26].

The numerical integration of Eq. (2) has been performed by use of the standard techniques of integration with respect to the Lévy-stable probability density function (PDFs) [11,16,27,28], leading to the following expression for the sample trajectories:

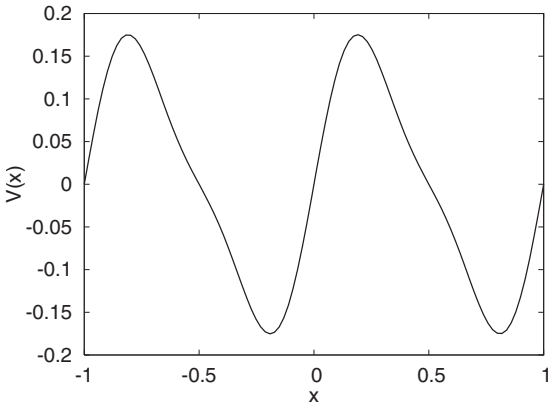

FIG. 1. The periodic potential $V(x)$ with a broken spatial symmetry used for inspection of the model ratchet system.

$$x(t)=x_0-\int_{t_0}^{t}V'(x(s))ds+\int_{t_0}^{t}\zeta(s)ds, \tag{3}$$

where

$$\int_{t_0}^{t}\zeta(s)ds=\int_{t_0}^{t}dL_{\alpha,\beta}(s)\approx\sum_{i=0}^{N-1}(\Delta s)^{1/\alpha}\zeta_i. \tag{4}$$

Here ζ_i are independent random variables distributed according to the stable probability density $L_{\alpha,\beta}(\zeta;\sigma,\mu)$ and $N\Delta s=t-t_0$. We assume that initially, at $t_0=0$, a test particle is located at $x=0$.

In the most general case Lévy distributions correspond to a four-parameter family of the probability density functions $L_{\alpha,\beta}(\zeta;\sigma,\mu)$; see [27–29]. The parameter α (where $\alpha\in(0,2]$) denotes the stability index of the distribution yielding (for $\alpha<2$) the asymptotic power law for the ζ distribution being proportional to $|\zeta|^{-(1+\alpha)}$. The parameter σ characterizes a scale (i.e., replacing the random variable ζ with $\sigma^{1/\alpha}\zeta$ rescales the argument of the distribution, but does not alter the distribution function itself), β defines an asymmetry (skewness), whereas μ denotes the location parameter. Throughout the paper we deal only with symmetric strictly stable distributions not exhibiting a drift; this implies a vanishing location and skewness parameters ($\mu=0$ and $\beta=0$) in the remaining part of this work. Accordingly, the characteristic function of the random stable variable ζ is given by a Fourier transform, $\phi(k)=\langle e^{ik\zeta}\rangle=\int_{-\infty}^{\infty}e^{ik\zeta}L_{\alpha,0}(\zeta;\sigma,0)d\zeta$, and reads

$$\phi(k)=\exp[-\sigma^{\alpha}|k|^{\alpha}]. \tag{5}$$

The parameter choice $\alpha=2$ corresponds to the Gaussian distribution and yields $\zeta(t)$ as the standard white, Gaussian noise of intensity $\sqrt{2}\sigma$; cf. Eq. (5). Figure 2 presents sample (symmetric) stable densities (top panel) with exemplary realizations of the process defined by Eq. (2). For illustrative purposes values of the stability index α have been set to 0.5, 1.0, 1.5, and 2.0. Notably, for a value of the stability index $\alpha<2$, the trajectories of the process defined by Eq. (2) are discontinuous. As α becomes smaller, larger jumps in the motion become more probable, reflecting the "fat tail" characteristics of the PDF describing statistics of random pushes.

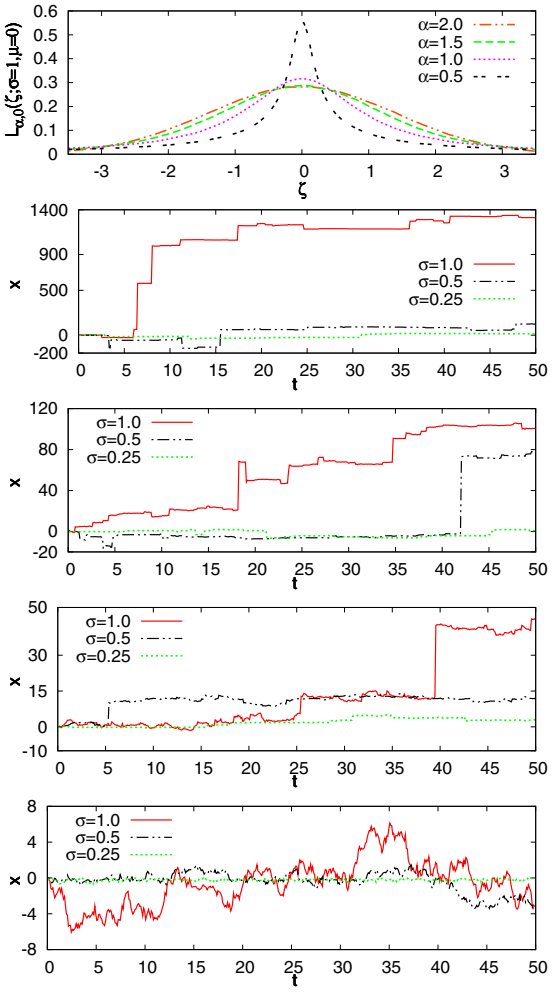

FIG. 2. (Color online) Sample symmetric stable densities (top panel) and exemplary realizations of the process given by Eq. (2) for the stability index $\alpha=\{0.5,1.0,1.5,2.0\}$ (from top to bottom). Various curves represent different scale parameters $\sigma=\{0.25,0.5,1.0\}$.

Note that the scale parameter σ scales the overall width of the PDF, $L_{\alpha,0}(\zeta;\sigma,0)=\sigma^{-\alpha}L_{\alpha,0}(\zeta/\sigma;1,0)$, and may be interpreted as the intensity of the external noise.

III. DETECTION OF PARTICLE CURRENT

For symmetric Lévy noises, Eq. (2) is equivalent to the following fractional differential Fokker-Planck equation [30–32]:

$$\frac{\partial P(x,t)}{\partial t}=\frac{\partial}{\partial x}V'(x)P(x,t)+\sigma^{\alpha}\frac{\partial^{\alpha}P(x,t)}{\partial|x|^{\alpha}}, \tag{6}$$

where the fractional (Riesz-Weyl) derivative is interpreted in the sense of the Fourier transform [21,22,33] $\frac{\partial^{\alpha}}{\partial|x|^{\alpha}}f(x)=-\int_{-\infty}^{\infty}\frac{dk}{2\pi}e^{-ikx}|k|^{\alpha}\hat{f}(k)$. Due to possible instabilities of numerical approximations [34,35] in the integration procedure of Eq. (6), in our studies we used an approach based solely on the Langevin equation (2). The numerical integration of Eq. (2) was performed with time step of $\Delta t=10^{-3}$. The number of realizations varied from $N=10^5$ to $N=10^6$, leading in all cases to consistent results.

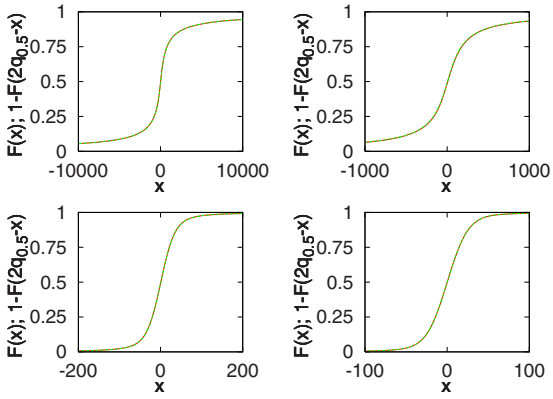

FIG. 3. (Color online) Cumulative distributions $F(x,t=100)$ and $1-F(2q_{0.5}-x,t=100)$ for $\alpha=0.7$ (top left panel), $\alpha=0.9$ (top right panel), $\alpha=1.5$ (bottom left panel), and $\alpha=1.7$ (bottom right panel) with $\sigma=1$. The perfect agreement between both curves indicates the symmetric shape of the corresponding PDFs with respect to the medians. The same agreement is observed for smaller values of the noise intensity σ. Note the large difference in scales for different values of α.

A test particle starts its motion from the position $x=0$. In the course of time the coordinate x changes due to the interplay of the stochastic driving and the action of the deterministic force; cf. Eq. (2). As we proceed to show, the ensuing coarse-grained probability distribution of x is a symmetric distribution with respect to its median of the power-law type (Sec. III A). The overall motion of the probability density is characterized by changes in the location of its median (Sec. III B). Moreover, the increasing width of PDFs is well reflected in growing interquantile distance (Sec. III C). Still other characteristics of the motion can be addressed by analyzing the behavior of the splitting probabilities: A particle initially located at $x=0$ can escape from an interval $[-L/2,L/2]$ to the left or to the right. The statistics of the corresponding escape events (splitting probabilities, Sec. III D) provides another measure of the directionality of motion. Finally, the mean escape time gives information about characteristic time scales involved in such escapes (Sec. III E).

A. Cumulative distribution

We first discuss the cumulative distribution function (CDF) of the particle's displacement under the nonequilibrium additive noise. The CDF is given by $F(x,t)=\int_{-\infty}^{x}P(x',t)dx'$ with $P(x,t)$ being the corresponding PDF, which can be interpreted in terms of the particle concentration. Our simulations show that in the course of time the corresponding PDF attains a symmetric form with respect to the medians; see Fig. 3. The density $P(x,t)$ is then found to move in one direction (towards the steeper slope of the potential) and to broaden in time. These effects can be seen by inspection of the overall position of the particles characterized by the median of the distribution $q_{0.5}(t)$ (cf. Fig. 6) and its width defined by the interquantile distance—

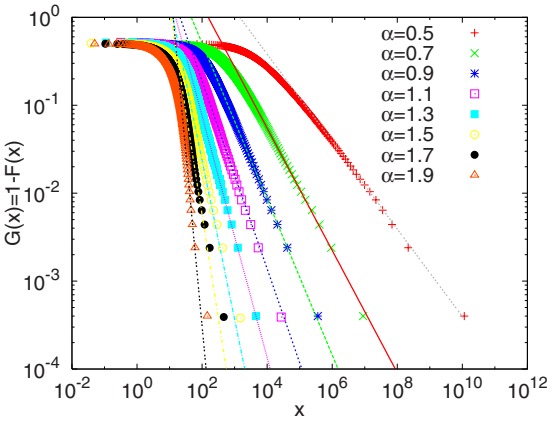

FIG. 4. (Color online) Survival probability $G(x,t=100)=1-F(x,t=100)$ estimated for $\sigma=1$.

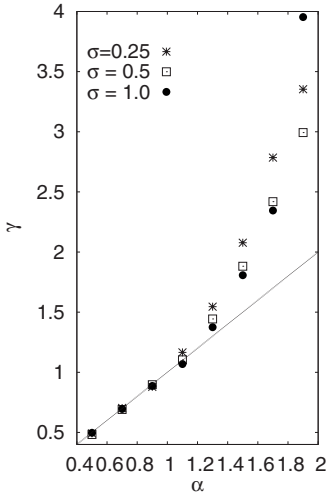

FIG. 5. Value of the exponent γ in the survival probability describing the asymptotic behavior of its tails $G(x,t)\propto x^{\gamma}$; see Fig. 4. Relative errors of the fit are smaller than 1% of the value of the exponents. Consequently, error bars are smaller than the symbol size.

e.g., $q_{0.8}(t)-q_{0.2}(t)$ (cf. Fig. 8). Here, the quantiles q_m $(0<m<1)$ of the probability distribution are defined according to the relation $F(q_m,t)=m$.

For symmetric probability densities—i.e., such that $P(q_{0.5}-x,t)=P(x+q_{0.5},t)$—the cumulative density $F(x,t)$ fulfills

$$F(x,t) = 1 - F(2q_{0.5} - x,t). \tag{7}$$

For the Lévy-ratchet system, the constructed CDFs prove that the PDF recorded at a given time is symmetric with respect to the median $(q_{0.5})$ if spatial scales much larger than the period of the potential $(L_x=1)$ are considered; cf. Figs. 1 and 3.

The distributions of the particle displacements in Fig. 3 exhibit power-law tails. In order to detect them it is sufficient to consider the asymptotic behavior of the "survival probability" $G(x,t)=1-F(x,t)$ defined in position space. For large x (see Fig. 4), this function clearly displays power-law behavior, $G(x,t)\propto x^{\gamma}$. The simplest hypothesis here could be that the corresponding exponent is the same as the one of the underlying noise. This kind of behavior is indeed observed for the values of stability index α smaller than or around 1; see Fig. 5. For larger values $\alpha>1.1$, $G(x,t)$ still exhibits a power-law asymptotics (see Fig. 4); however, the numerically obtained values of the exponents γ differ significantly from α; see Fig. 5. This difference is pertinent to a very far tail of the distribution, since the behavior of the interquantile distances, say $q_{0.8}(t)-q_{0.2}(t)$, unveils the behavior compatible with the $\gamma=\alpha$ assumption for all α; see Sec. III C.

Inspection of the survival probability $G(x,t)$ (see Fig. 4) suggests that for small values of α the particle practically does not feel the potential. Accordingly, for free superdiffusive motion [see Eq. (2)] the exponent characterizing the survival probability is the same as the one characterizing the statistical properties of the noise. This observation is in agreement with the predictions of the continuous-time random-walk theory for situations when the mean waiting time for the next jump is finite [36,37]. For increasing values of α, the motion becomes more sensitive to the structure of the potential. Consequently, the form of $G(x,t)$ in the intermediate range of x departs from the pure Lévy distribution. The difference between γ and α can be most likely explained by extremely slow convergence of the tail of the corresponding distribution to its asymptotic form.

In order to fit the tail asymptotics properly, it is necessary to collect large statistics corresponding to extreme events which should cover at least a couple of orders of magnitude. Such an accumulation of data is easily achievable for values of $\alpha\leqslant 1.1$. In contrast, for larger values of the stability index α $(\alpha>1.1)$, the investigation of x asymptotics requires extremely long simulation times, which make the task of building sufficient $G(x,t)$ statistics infeasible. The values of γ obtained in simulations did not indicate changes for chosen simulation times; however, the fitted slope was found to be sensitive to the choice of the threshold from which the power law was fitted.

B. Median and group velocity

The position of the median describes the overall motion of the probability density of finding a particle in the vicinity of x. In our case, the corresponding PDF, coarse-grained over the period of the potential, is a symmetric, monomodal function. Therefore, the temporal change of the median (which coincides with the maximum of the PDF) allows one to define the group velocity of the particle packet as the time derivative of the median $dq_{0.5}/dt$. Our numerical simulations show that the position of the median $q_{0.5}(t)$ changes linearly with time,

$$q_{0.5}(t) = vt + b, \tag{8}$$

which corresponds to the constant group velocity v. Note that the parameter $dq_{0.5}/dt$ describing the group displacement of test particles can be defined even in those cases when, due to large fluctuations, the average current does not exist. Figure 6 presents the location of the median as a function of time for different values of the stability exponents α.

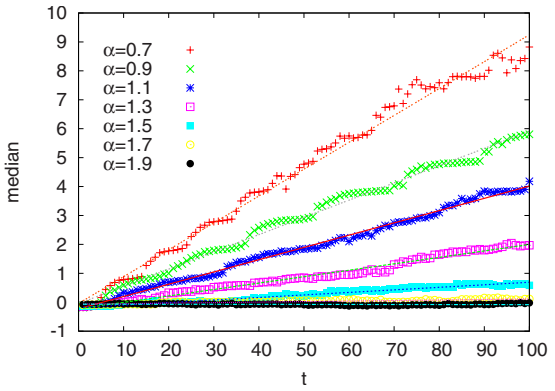

FIG. 6. (Color online) Time dependence of the location of median, $q_{0.5}(t)$, which describes the overall motion of the ensemble of particles. Sample trajectories have been numerically estimated from Eq. (2) for $\sigma=1$.

The "periodiclike" modulation of the median position is caused by the periodic shape of the potential; see the ordinate of Fig. 1. For the constant amplitude of the noise the group velocity decreases with increasing stability exponent α and disappears in the Gaussian case $\alpha=2$; see Fig. 7. In this limiting case the Langevin equation (2) models an overdamped Brownian motion in an external potential under the influence of a thermal heat bath. In the long-time limit, the so-called reduced probability density for this model [4],

$$\tilde{P}(x,t) = \sum_{n=-\infty}^{+\infty} P(x + nL_x, t), \tag{9}$$

approaches a steady state which correctly reproduces the Boltzmann distribution

$$\tilde{P}(x) = Z^{-1} e^{-V(x)/\sigma^2}, \tag{10}$$

where

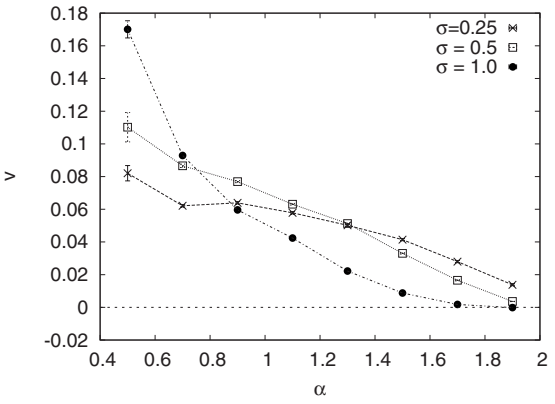

FIG. 7. Value of the group velocity [cf. Eq. (8) and Fig. 6] as a function of the stability index α. The lines are drawn to guide the eye. The fastest overall motion of the probability density is observed for small values of the stability index α for which large noise increments are more probable. Error bars, except for those for $\alpha=0.5$, are smaller than the symbol size.

$$Z = \int_0^{L_x} dx e^{-V(x)/\sigma^2}, \tag{11}$$

and the average particle current $\langle \dot{x} \rangle$ vanishes; i.e., in spite of the broken spatial symmetry, there arises no systematic preferential motion.

In contrast, for $\alpha<2$, the group velocity is positive; see Figs. 6 and 7. This clearly indicates the preferred directed motion: the test particles are climbing "uphill" along a steeper slope of the potential. The situation therefore resembles the standard temperature ratchet model, in which the temperature variations, being stochastic or time periodic, give rise to the net transport [2,4,5] in the same direction. The physical interpretation of this effect, at least at weak noises, is related to the observation that unlike for a regular Gaussian diffusion, the dynamics driven by Lévy white noise is determined by large jumps whose intensity and sizes are controlled by tails of the density $|\zeta|^{-(1+\alpha)}$ [38]. At the beginning, the particles reside close to the minimum of the potential $V(x)$ awaiting large enough noise pulses to be catapulted out. Such strong pulses throw the particle with equal probability to the left or to the right. After experiencing the pulse, most of the particles land on the longer and flatter slopes of the potential landscape, and continue a more regular diffusive motion; i.e., most of the catapulted particles indeed move to the right until they are captured again in the minima of the potential. This gives rise to the overall preferred motion to the right. We see that the mechanism of rectification is quite similar to the one in a thermal ratchet where during the cooldown period, particles diffuse a long distance to the right and a short distance to the left.

C. Interquantile distance

The interquantile distance is a robust measure characterizing the spread of a distribution (distribution's width), also in situations when the moments of this distribution do not exist. Numerical simulations performed on our model Lévy ratchet indicate that the interquantile distance scales such as t^p:

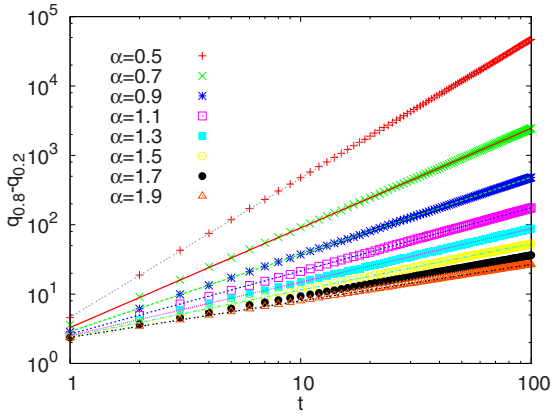

FIG. 8. (Color online) Time dependence of the interquantile distance $q_{0.8}(t)-q_{0.2}(t)$ for $\sigma=1$. Lines passing through the data points represent fitted curves; see Eq. (12).

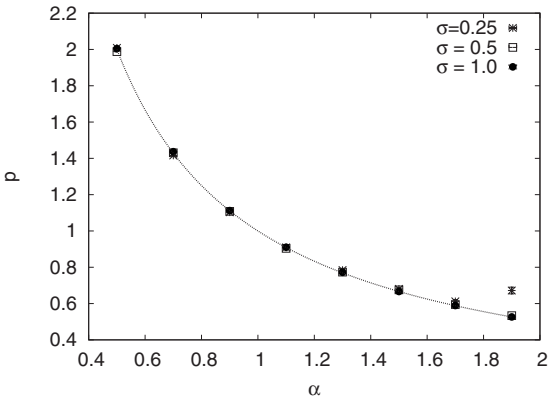

FIG. 9. Value of the exponent p in Eq. (12) as a function of the stability index α. The line drawn through the points presents the dependence of the exponent characterizing the growth of the interquantile distance for the free-particle case, $V(x)=0$—i.e., $p=1/\alpha$. Error bars are smaller than the symbol size.

$$q_m(t) - q_{1-m}(t) \propto t^p, \tag{12}$$

where $p=1/\alpha$. Figure 8 presents the time dependence of the interquantile range $q_{0.8}(t)-q_{0.2}(t)$ fitted to Eq. (12) for $\sigma=1$. At lower values of σ some sensitivity of the statistics to the shape of the potential is registered, giving rise to periodiclike modulation of the interquantile distances (results not shown). In Fig. 9 resulting values of the fitted exponents are displayed, indicating the $1/\alpha$ behavior for three different values of the noise intensity σ. Notably, the interquantile range $q_m(t)-q_{1-m}(t)$ scales in the same manner also for other values of m $(0<m<1)$ (results not shown). Our numerical analysis indicates that, typically, the periodic modulation which has been observed in the time evolution of the median is no longer detectable in the interquantile distance. Essentially, this observation remains true for any quantiles $q_m(t)$ with $m\neq 0.5$ and for sufficiently high noise intensities $\sigma \geqslant 1$. This kind of behavior is weakened, however, for lower intensities σ when the shape of the potential induces periodic modulation in the interquantile range (results not shown).

D. Splitting probability

Yet another characteristics of the directionality of the motion can be given by considering so-called splitting probabilities. Let us introduce an interval $[-L/2,L/2]$ in the neighborhood of $x=0$ where the particle initially resides. We analyze the statistics of trajectories escaping this interval through its left or right boundary. The splitting probability π_L gives us the fraction of first escape events through the left boundary and is displayed in Fig. 10 as a function of the box half-width $L/2$. The statistics of first escapes π_L clearly indicates the preferred direction of the motion to the right, since for larger intervals $\pi_L<1/2$. This tendency becomes stronger at lower values of the scale parameter σ.

Figure 10 depicts a clear difference between the situations $1<\alpha<2$ and $\alpha<1$. In the first case, for intervals ("boxes") much larger than the period of the potential $L_x=1$, the probability π_L decays monotonously with the box size. This observation suggests that more and more particles leave the box $[-L/2,L/2]$ through its right boundary. In contrast, for $\alpha<1$ the behavior of π_L is nonmonotonous: it decays with $L/2$ up to $L/2\approx 20$ and then it starts to grow again.

This striking difference between the results for $\alpha>1$ and ones for $\alpha<1$ can be understood when returning to the discussion of interquantile distances. For $\alpha>1$ the shift of the distribution's median (coinciding with its maximum) increases linearly in time and this enlargement is asymptotically faster than the growth of the distribution's width. In consequence, the mean position of the particle $\langle x\rangle$ and the average current $\langle \dot{x}\rangle$ are well-defined quantities. In the course of time the typical displacement (the mean position) wins over the spread, and most of the particles come out of the box through its right boundary.

This situation changes for $\alpha<1$ when the width of the distribution grows faster than its maximum moves. Due to the well-prescribed initial position, the contribution of the

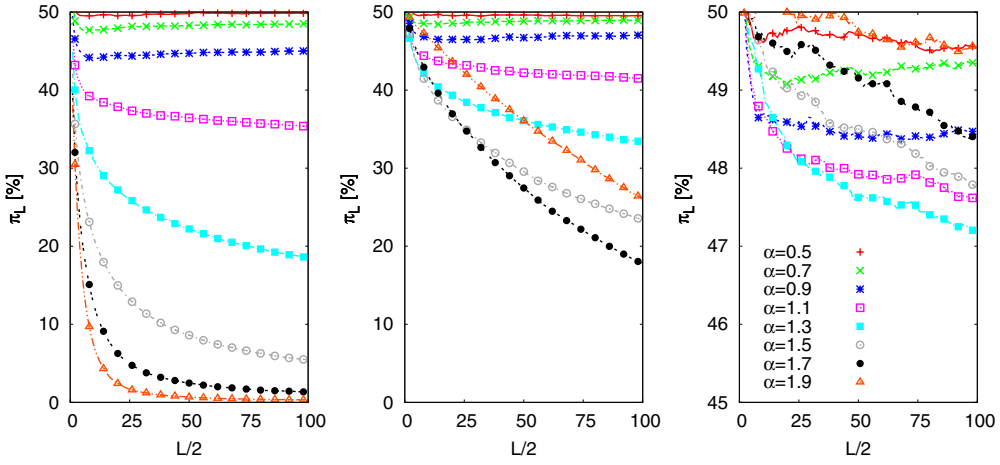

FIG. 10. (Color online) Splitting probability π_L—i.e., probability of the first escape to the left as a function of the box half-width. Initially the particle is located at $x=0$. Various panels correspond to different values of the scale parameter σ: $\sigma=0.25$ (left panel), $\sigma=0.5$ (middle panel), and $\sigma=1$ (right panel).

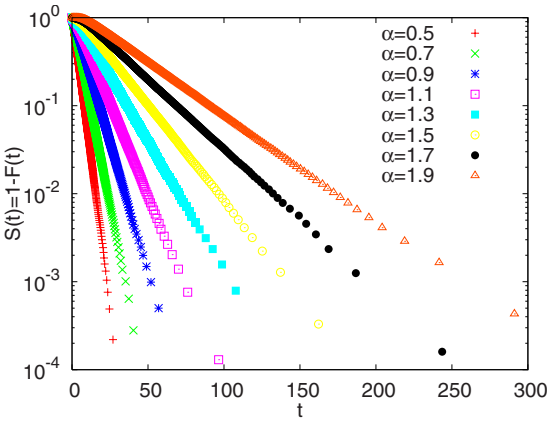

FIG. 11. (Color online) Survival probability $S(t)=1-F(t)$—i.e., the probability of finding a particle in the box of the width $L=10$ at time t. In simulations the noise intensity $\sigma=1$ has been used.

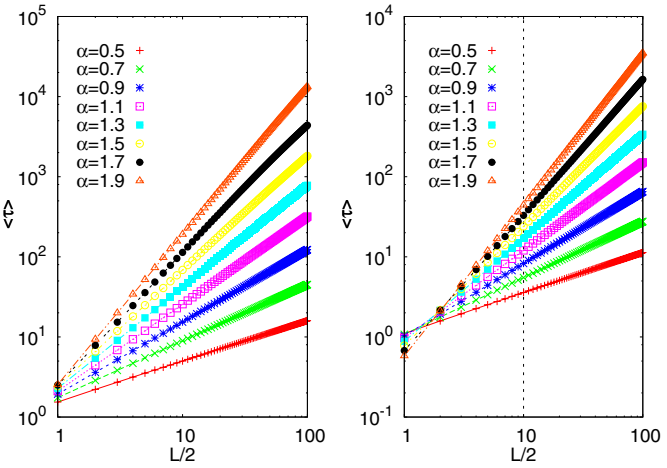

FIG. 12. (Color online) Mean exit time $\langle\tau\rangle$—i.e., the average of the escape time from the box as a function of the box half-width for $\sigma=0.5$ (left panel) and $\sigma=1$ (right panel).

overall motion is still perceptible in statistical analysis at shorter times and for smaller boxes. Accordingly, the difference between the probabilities to leave the box through its left versus right boundary increases. At longer times the broadening of the distribution prevails, a typical (mean) displacement gets hardly relevant on the background of fluctuations, and the difference between the splitting probabilities decays. However, the PDF still has a pronounced maximum, and the derivative of its time-dependent location defines the group velocity.

E. Exit time

Next, we investigate the quantity closely related to the splitting probability—i.e., the mean escape time from the $[-L/2,L/2]$ box. Here we analyze the escape time τ, defined as the exit time through either one of the box boundaries. This exit time is equivalent to the first passage time from the starting point $x(0)$ to the left or to the right absorbing boundary located at $x=\pm L/2$. Note that the boundary conditions associated with the Lévy-type motion are nonlocal. In consequence, not only the edges, but also two exterior semilines outside the interval have to be absorbing [16].

The same information which is carried by the escape time distribution can be also deduced from the analysis of the survival probability. By definition, the survival probability $S(t)=1-F(t)$ is the probability of finding a particle in a given box interval at time t; i.e., it pertains to the fraction of particles which still remain in the box at time t. The survival probability $S(t)$ for the Lévy-noise-driven diffusion in external potentials has been shown to be exponential within the range of moderate and high potential barriers [16,20,39,40]. At noise intensities $\sigma\approx 1$, the deviations from the exponential character of survival distribution are observed for low barrier heights when the particle motion approaches a free superdiffusion case [16].

In Fig. 11, survival probabilities are depicted for the set of parameters $\sigma=1$, $L=10$ illustrating exponential-like behavior of this quantity for various values of the stability index α. The similar $S(t)$ dependence has been recorded for other values of the box width L and scale parameter σ (results not shown).

Using the statistics of escape times it is possible to evaluate the mean exit time. For a free particle starting its motion at the center of the interval $[-L/2,L/2]$ the analytical formula for the mean exit time is known [17] and reads

$$\langle\tau(x(0)=0)\rangle=\frac{(L/2)^{\alpha}}{\sigma^{\alpha}\Gamma(\alpha+1)}. \tag{13}$$

By taking this formula as a hypothetical relation

$$\langle\tau(x(0)=0)\rangle=a\left(\frac{L}{2}\right)^{b}, \tag{14}$$

it is possible to test the break down of this kind of scaling in numerical estimation of $\langle\tau\rangle$ for the Lévy ratchet. As can be inferred by inspection of Fig. 12, for large values of the scale parameter σ (representing the intensity of the noise), the presence of the potential does not affect the kinetics of a particle. Accordingly, both the prefactor a and the exponent b in Eq. (14) are the same as for the free-particle case—i.e., $a=1/[\Gamma(\alpha+1)\sigma^{\alpha}]$ and $b=\alpha$. Notably, the main contribution to the mean exit time $\langle\tau\rangle$ comes in this case from the $(L/2)^b$ term; see Eq. (13). The prefactor in Eq. (13) slightly modifies only this dependence. Consequently, the intersection of $\langle\tau\rangle$ curves visible in the right panel of Fig. 12 reflects properties of the power-law function $(L/2)^b$ for arguments $L/2$ smaller and larger than two. The dominance of the scaling $\langle\tau\rangle\propto(L/2)^b$ explains also different behavior of $\langle\tau\rangle$ for $L<2$ and $L>2$. Namely, for $L<2$ the shortest mean exit times are observed for large α. Contrariwise, for $L>2$ the shortest mean exit times are recorded for small values of α; see right panel of Fig. 12. At lower noise intensities this effect disappears as can be observed in the left panel of Fig. 12.

Lowering noise intensity σ changes the scaling $b\neq\alpha$ and the prefactor a in Eq. (14). The discrepancy between the theoretical result, Eq. (13), for the free-particle case and the numerical estimate becomes clearly visible when the driving Lévy noise approaches a Gaussian limit ($\alpha\approx 2$) and the noise

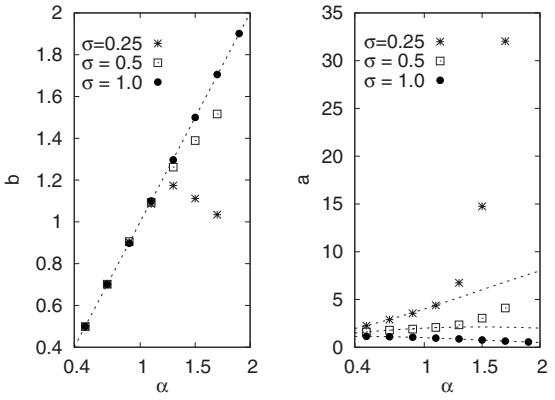

FIG. 13. Value of the exponent b and the prefactor a in Eq. (14) as a function of the stability index α. Lines present theoretical values of the exponent and the prefactor characterizing mean escape time for a free particle—i.e., α and $1/[\Gamma(\alpha+1)\sigma^{\alpha}]$, respectively.

intensity weakens (see Fig. 13). Nevertheless, for small to moderate values of the stability index α and within the considered range of the noise intensities ($\sigma \in \{0.25, 0.5, 1\}$), the escape time in the minimal Lévy-ratchet system follows the law derived for a free-superdiffusion case.

IV. SUMMARY AND CONCLUSIONS

In the foregoing sections we have introduced a model which operates as a minimal Lévy-noise-driven ratchet. We have numerically documented that the motion of the overdamped particle subjected to a symmetric Lévy white noise in a potential with a broken spatial symmetry leads to the occurrence of directionality of motion. The preferred direction of motion results as a consequence of an interplay between the nonequilibrium character of the underlying stable noise and the broken spatial symmetry of the static potential.

Lévy white noise constitutes an interesting generalization of ordinary white Gaussian noise, which is understood as a time derivative of a stationary Brownian walk process with independent increments. Unlike the case of ordinary Brownian motion (mathematically described as a Wiener process), the Lévy-Wiener process under a constant force does not exhibit a Gibbsian "nature" of the long-time distribution. Moreover, although it is stationary and its increments are also statistically independent, their step size is drawn from a Lévy distribution characterized by the stability index $0<\alpha<2$. The Lévy distribution has a long-range algebraic tail corresponding to large but infrequent steps. For $\alpha<2$ this distribution has the interesting property that the central-limit theorem does not hold in its usual form. In particular, the mean-square-step deviation for the Lévy-Wiener process diverges and the rare large-step events prevail determining the long-time behavior leading to anomalous enhanced "superdiffusion." Accordingly, typical characteristics of motion such as the particle displacement or mean velocity and a diffusion coefficient, become ill defined. This situation calls for introducing other robust statistical measures of the directed motion. Our approach based on detailed computer simulations allows us to study the collective motion of Lévy-Brownian particles by analyzing the group velocity, interquantile width of the displacement distribution, and survival and splitting probabilities.

In our model system, initially a sharp distribution of particle positions, broadens in the course of time, leading to a symmetric (with respect to its median) probability density of the power-law type. The median of this distribution, which characterizes the group velocity of the particle packet, moves linearly with time, exhibiting the fastest motion for small values of the stability exponent α. The coherence of such motion has been further characterized by the interquantile width of the distribution of particle position. For $\alpha>1$ the width of the distribution has been shown to grow slower than its maximum moves, contrary to the situation when $0<\alpha<1$. This fact has been reflected in the behavior of splitting probabilities for leaving an interval of a given length.

Notably, the increase of the stability index α decreases the ratcheting effect. In particular, for $\alpha=2$, similarly to the original ratchet-and-pawl device [4], the absence of the average particle current is a simple consequence of the second law of thermodynamics: despite the broken spatial symmetry assured by the form of the potential, no systematic preferential motion of the random dynamics can be detected and the rectifying effect disappears.

In a Lévy ratchet, a combination of a symmetric stable noise and a periodic potential with broken spatial symmetry provides a minimal sufficient setup for the occurrence of directed current. However, contrary to Gaussian noises, stable Lévy ones can be intrinsically asymmetric and such a modification of the noise pulses affects the particle current [13]. Moreover, a cyclic variation of the asymmetry parameter may modify the Lévy ratchet between a "thermal" or a "tilting" type. We assume that considering such situations might be an interesting further step pursuing our line of investigations.

ACKNOWLEDGMENTS

The authors acknowledge stimulating and inspiring discussions with E. Barkai and I. Pavlyukevich. This research has been supported by a Marie Curie TOK COCOS grant (6th EU Framework Program under Contract No. MTKD-CT-2004-517186) and the European Science Foundation (ESF) via "Stochastic Dynamics: fundamentals and applications" (STOCHDYN) program. Additionally, B.D. acknowledges support from the Foundation for Polish Science and the hospitality of the Humboldt University of Berlin and the Niels Bohr Institute (Copenhagen). The support of DFG within SFB555 is also acknowledged.

[1] R. D. Astumian and M. Bier, Phys. Rev. Lett. **72**, 1766 (1994).
[2] M. O. Magnasco, Phys. Rev. Lett. **71**, 1477 (1993).
[3] J. Kula, T. Czernik, and J. Łuczka, Phys. Rev. Lett. **80**, 1377 (1998).
[4] P. Reimann, Phys. Rep. **361**, 57 (2002).
[5] P. Reimann and P. Hänggi, Appl. Phys. A: Mater. Sci. Process. **75**, 169 (2002).
[6] *Lévy Flights and Related Topics in Physics*, edited by M. F. Shlesinger, G. M. Zaslavsky, and J. Frisch (Springer-Verlag, Berlin, 1995).
[7] *Lévy Processes: Theory and Applications*, edited by O. E. Barndorff-Nielsen, T. Mikosch, and S. I. Resnick (Birkhäuser, Boston, 2001).
[8] A. A. Dubkov and B. Spagnolo, Fluct. Noise Lett. **5**, L267 (2005).
[9] A. A. Dubkov and B. Spagnolo, Acta Phys. Pol. B **38**, 1745 (2007).
[10] B. Dybiec and E. Gudowska-Nowak, Phys. Rev. E **69**, 016105 (2004).
[11] B. Dybiec and E. Gudowska-Nowak, Fluct. Noise Lett. **4**, L273 (2004).
[12] B. Dybiec and E. Gudowska-Nowak, Acta Phys. Pol. B **37**, 1479 (2006).
[13] B. Dybiec and E. Gudowska-Nowak, New J. Phys. **9**, 452 (2007).
[14] B. Dybiec, Ph.D. thesis, Jagellonian University, 2005.
[15] A. V. Chechkin *et al.*, J. Stat. Phys. **115**, 1505 (2004).
[16] B. Dybiec, E. Gudowska-Nowak, and P. Hänggi, Phys. Rev. E **73**, 046104 (2006).
[17] A. Zoia, A. Rosso, and M. Kardar, Phys. Rev. E **76**, 021116 (2007).
[18] P. D. Ditlevsen, Phys. Rev. E **60**, 172 (1999).
[19] A. Chechkin, V. Gonchar, J. Klafter, and R. Metzler, Europhys. Lett. **72**, 348 (2005).
[20] B. Dybiec, E. Gudowska-Nowak, and P. Hänggi, Phys. Rev. E **75**, 021109 (2007).
[21] A. V. Chechkin *et al.*, Chem. Phys. **284**, 233 (2002).
[22] A. V. Chechkin, J. Klafter, V. Y. Gonchar, R. Metzler, and L. V. Tanatarov, Phys. Rev. E **67**, 010102(R) (2003).
[23] B. Dybiec, E. Gudowska-Nowak, and I. M. Sokolov, Phys. Rev. E **76**, 041122 (2007).
[24] D. del Castillo-Negrete, V. Gonchar, and A. Chechkin, e-print arXiv: 0710.0883.
[25] D. Brockmann and I. M. Sokolov, Chem. Phys. **284**, 409 (2002).
[26] B. West and V. Seshadri, Physica A **113**, 203 (1982).
[27] A. Janicki and A. Weron, *Simulation and Chaotic Behavior of α-Stable Stochastic Processes* (Dekker, New York, 1994).
[28] A. Janicki, *Numerical and Statistical Approximation of Stochastic Differential Equations with Non-Gaussian Measures* (Hugo Steinhaus Centre for Stochastic Methods, Wrocław, 1996).
[29] W. Feller, *An Introduction to Probability Theory and its Applications* (Wiley, New York, 1968).
[30] R. Metzler, E. Barkai, and J. Klafter, Europhys. Lett. **46**, 431 (1999).
[31] V. V. Yanovsky, A. V. Chechkin, D. Schertzer, and A. V. Tur, Physica A **282**, 13 (2000).
[32] D. Schertzer *et al.*, J. Math. Phys. **42**, 200 (2001).
[33] S. Jespersen, R. Metzler, and H. C. Fogedby, Phys. Rev. E **59**, 2736 (1999).
[34] M. M. Meerschaert and C. Tadjeran, J. Comput. Appl. Math. **172**, 65 (2004).
[35] R. Gorenflo *et al.*, Chem. Phys. **284**, 521 (2002).
[36] R. Metzler and J. Klafter, Phys. Rep. **339**, 1 (2000).
[37] R. Metzler and J. Klafter, J. Phys. A **37**, R161 (2004).
[38] P. Imkeller and I. Pavlyukevich, J. Phys. A **39**, L237 (2006).
[39] P. Imkeller and I. Pavlyukevich, Stochastic Proc. Appl. **116**, 611 (2006).
[40] A. Malakhov and A. Pankratov, Adv. Chem. Phys. **121**, 357 (2002).